

RUGGED a-Si:H TFTs ON PLASTIC SUBSTRATES

H. GLESKOVA¹, S. WAGNER¹, Z. SUO²

Princeton University, ¹Department of Electrical Engineering, and ²Department of Mechanical and Aerospace Engineering and Princeton Materials Institute, Princeton, NJ 08544

ABSTRACT

Much of the mechanical strain in semiconductor devices can be relieved when they are made on compliant substrates. We demonstrate this strain relief with amorphous silicon thin-film transistors (a-Si:H TFTs) made on 25- μm thick polyimide foil, which can be bent to radii of curvature R down to 0.5 mm without substantial change in electrical characteristics. At $R = 0.5$ mm the channel area of the TFTs is strained by $\sim 1\%$. The reduction in bending radius, from $R = 2$ mm on steel foil of the same thickness, agrees with the theoretical prediction that changing from a stiff to a compliant substrate can reduce the bending strain in the device plane by a factor of up to 5.

INTRODUCTION

The main failure mechanism of laptop computers, cellular phones and similar portable devices is breakage of the glass of the display. To solve this problem much research is focused on the fabrication of thin-film electronics on plastic substrates [1-8]. Plastic substrates have Young's moduli about 100 times smaller than those of glass or stainless steel, and therefore are flexible. Their flexibility makes them ideal for roll-to-roll processing and also for large-area flexible electronics. However, the transition from glass to plastic substrates has important consequences for fabrication and mechanical performance. For example, the glass transition temperature of most plastics lies below 200°C, which restricts the maximum process temperature to $\leq 150^\circ\text{C}$. Due to the lower Young's modulus of plastic substrates, the mechanical behavior of the circuits fabricated on them is different from that on the rigid glass substrates. We have analyzed theoretically this transition from stiff to compliant substrate materials [9]. Here we report measurements that show to what extent amorphous silicon (a-Si:H) thin-film transistors (TFTs) made on polyimide foil indeed are insensitive to rolling and bending.

In a thin-film circuit / substrate couple, the substrate becomes compliant when its stiffness becomes comparable to the stiffness of the circuit films. Because Young's moduli Y_f of the a-Si:H TFT materials are ~ 200 GPa, Young's modulus Y_s of the polyimide Kapton E is ~ 5 GPa, and the film thickness d_f typically is ~ 1 μm , the compliant condition is established for substrate thickness $d_s \leq 300$ μm . To test this condition, we have made a-Si:H TFTs on 1-mil (25 μm) thick Kapton E foils. A series of mechanical tests performed on the TFTs in conjunction with their electrical evaluation indeed demonstrate their extraordinary ruggedness.

TRANSISTOR FABRICATION

Because the glass transition temperature of plastics ($\leq 200^\circ\text{C}$) is much lower than that of the conventional substrates, Corning 7059 and 1737 glass ($\geq 600^\circ\text{C}$), the deposition of all a-Si:H TFT layers had to be re-optimized for 150°C to achieve electrical properties comparable to

those obtained at the conventional process temperature of 250°C to 350°C [2]. All silicon layers were deposited using a three-chamber rf-excited plasma enhanced chemical vapor deposition system. The gate SiN_x was deposited from a mixture of SiH_4 , NH_3 and H_2 , the undoped a-Si:H from a mixture of SiH_4 and H_2 , and the (n^+) a-Si:H from a mixture of SiH_4 , PH_3 and H_2 .

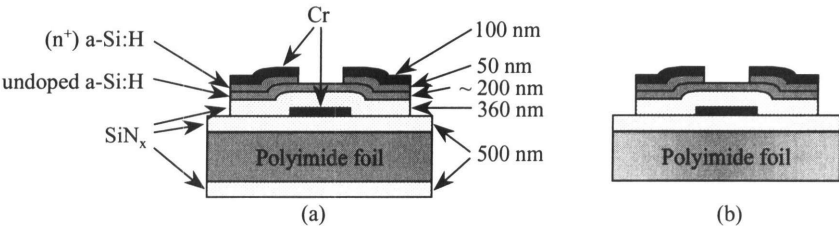


Fig. 1. Cross-section of a-Si:H TFT on 25 μm thick Kapton foil. (a) As-fabricated sandwich structure; (b) Back SiN_x removed for the bending tests of Fig. 4.

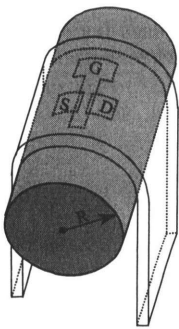


Fig. 2. TFT bent inward.

The TFTs have the bottom gate, back-channel etch structure shown in Fig. 1. We began by passivating a 25- μm -thick Kapton E substrate on both sides with 0.5 μm thick layers of SiN_x . These layers serve as a barrier against the solvents, bases and acids used during photolithography. An ~ 100 nm thick Cr layer was thermally evaporated and wet etched to create the gate electrode. The TFT sequence was 360 nm of SiN_x , ~ 200 nm of undoped a-Si:H, and ~ 50 nm of (n^+) a-Si:H. An ~ 100 nm thick Cr layer was thermally evaporated. We wet etched the Cr source-drain pattern and dry etched the (n^+) a-Si:H in CF_4 gas. Then the undoped a-Si:H was dry etched to define the transistor island. In the last photolithographic step, we dry etched windows into the SiN_x to open access to the gate contact pads. Arrays of TFTs with gate length $L = 15 \mu\text{m}$ and width $W = 210 \mu\text{m}$ were fabricated on 1.5 x 1.5 sq. in. substrates. Four substrates were processed simultaneously.

The as-fabricated TFT/substrate structure had a built-in radius of curvature R of 18 mm, with the TFTs on the outside, showing that the as-fabricated transistors were under compressive stress. Before bending the TFTs we removed the stiff SiN_x layer from the back of the substrate. This reduced the radius of curvature of the structure to 8 mm, with the TFTs still on the outside. The stiff SiN_x layer on the back of the substrate stiffens the whole structure, thus masking the compliancy of the plastic substrate. Removing the back SiN_x layer renders the plastic truly compliant. (See the Results and Discussion section for further discussion.)

Individual transistors were stressed mechanically by bending inward (the devices facing in), which is shown schematically in Fig. 2, or outward (the devices facing out). Single TFTs were bent to decreasing R , beginning with $R = 4$ mm down to $R = 0.5$ mm. The TFT was stressed for one minute at each bending radius, and then was released and remeasured.

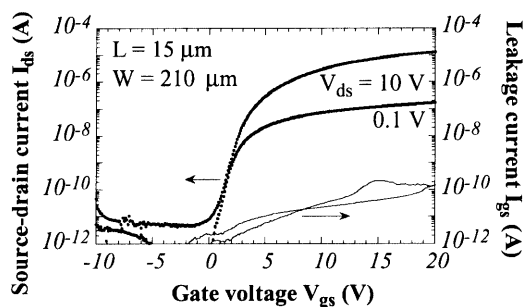


Fig. 3. Transfer characteristics of *a*-Si:H TFT on 25 μm thick Kapton.

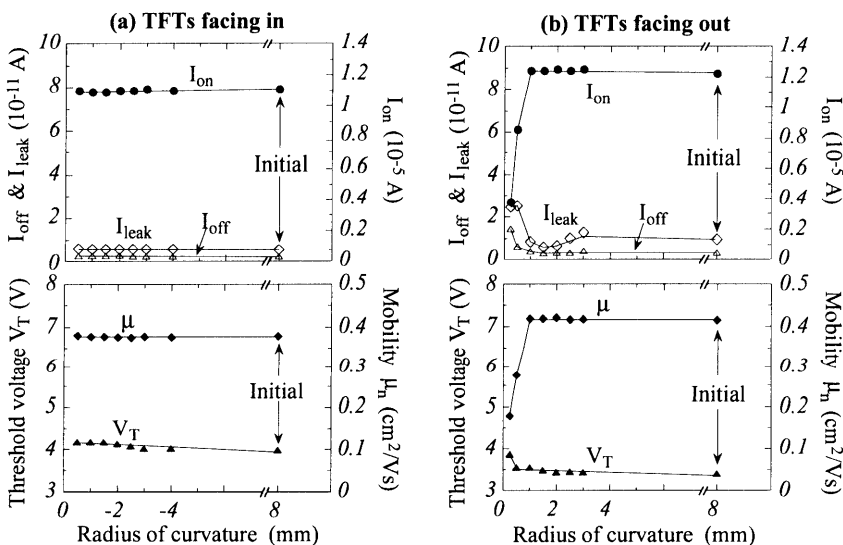


Fig. 4. On-, source-gate leakage, off-currents, electron mobility, and threshold voltage in the saturation regime as functions of bending radius. The initial, built-in radius is 8 mm. Outward bending R is defined positive, inward bending negative. Differences between the "Initial" characteristics reflect spread between as-fabricated TFTs.

RESULTS AND DISCUSSION

a-Si:H TFT Performance Upon Bending

The TFT transfer characteristics I_{ds} vs. V_{gs} , for $V_{ds} = 0.1$ V and 10 V, are shown in Fig. 3. The off-current is $\sim 5 \times 10^{-12}$ A ($\sim 2.4 \times 10^{-14}$ A/ μm) and the on-off current ratio is $> 10^6$.

In the saturation regime the source-drain current is given by:

$$I_{ds} = \mu_n C_{SiN} \frac{W}{2L} (V_{gs} - V_T)^2 \quad (1)$$

where μ_n is the effective electron mobility, C_{SiN} the capacitance of the gate insulator, W the channel width, L the channel length, V_{gs} the gate voltage, and V_T the threshold voltage. The dielectric constant of our 150°C nitride measured at 1 MHz is 7.46 and we calculate $C_{SiN} = 1.83 \times 10^{-8} \text{ F cm}^{-2}$. At $V_{ds} = 10 \text{ V}$ we obtain $V_T \sim 2.7 \text{ V}$ and a saturated mobility of $\sim 0.4 \text{ cm}^2 \text{ V}^{-1} \text{ s}^{-1}$ for the TFT of Fig. 3.

Fig. 4 summarizes the results of the inward (a) and outward (b) bending tests performed on TFTs fabricated on 25 μm thick Kapton foil. The top graphs show the on-current I_{on} , the off-current I_{off} , and the gate-leakage current I_{leak} as functions of the radius of curvature. The definition of these currents is as follows: the off-current is the smallest source-drain current at $V_{ds} = 10 \text{ V}$, the on-current is the source-drain current for $V_{ds} = 10 \text{ V}$ and $V_{gs} = 20 \text{ V}$, and the leakage current is the source-gate current for $V_{ds} = 10 \text{ V}$ and $V_{gs} = 20 \text{ V}$. No change in these parameters for bending down to $R = 0.5 \text{ mm}$ was observed for inward bending and only a minor change for $R \leq 0.5 \text{ mm}$ for outward bending. For outward bending we also show some data for $R = 0.25 \text{ mm}$ but these should be taken with some reservation because the radius of 0.5 mm was the smallest controlled value we could set reliably. The bottom graphs show the threshold voltage V_T and the saturated electron mobility μ_n , calculated using Eq. (1), as a function of the bending radius. The slight monotonous rise in the threshold voltage, observed in both cases, does not result from bending because a similar shift was observed also in repeated measurements of unstressed TFTs. The mobility remains constant for inward bending, but for outward bending a decrease is observed for $R \leq 0.5 \text{ mm}$. No catastrophic failure occurs.

Strain in the Channel of the TFT

Both the fabrication process and the externally applied bending moment cause strain in the TFT structure. The difference in the coefficient of thermal expansion between Kapton and the TFT layers, and strain built in during deposition cause the as-fabricated TFTs to be under compressive strain (the radius of curvature of the substrate, coated on both sides with SiN_x , is 18 mm and the TFTs are on the outside). Let us analyze the TFTs when we bend them inward. In that case the TFTs are put under additional compressive strain. We calculate the strain that is produced during our bending experiment in the channel of the TFT. For the calculation of this additional strain we assume that the as-fabricated structure is free of strain. Therefore, the structure is assumed to be flat before the external bending moment is applied. The substrate has thickness d_s and Young's modulus Y_s . It is covered on both sides with stiff films with Young's modulus Y_f and thicknesses d_{f1} and d_{f2} , as shown in Fig. 5.

When an external bending moment is applied to this structure, the film on the outside is under tension while the film on the inside is under compression. Geometry dictates that the strain ϵ_x in the bending direction x is linear in z , namely,

$$\epsilon_x = z / R \quad (2)$$

because the neutral plane is free of strain [9]. Here R is the radius of curvature and z is measured from the neutral plane. Each layer of the material is taken to be an isotropic elastic solid with Young's modulus Y . The film and the substrate are dissimilar materials, and Y is a

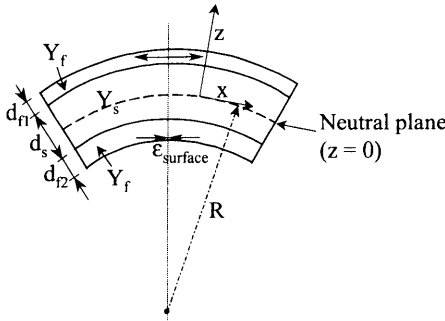


Fig. 5. Films-on-foil structure bent to a cylindrical roll.

This allows us to calculate the strain $\epsilon_{surface}$ on the surface of the TFT film (the inside film) using Eq. (2), namely,

$$\epsilon_{surface} = \frac{d_s + d_{f1} + d_{f2}}{2R} \cdot \frac{\chi(\eta_1^2 + \eta_2^2) + 2(\chi\eta_1 + \chi\eta_1\eta_2 + \eta_2) + 1}{\chi(\eta_1 + \eta_2)^2 + (\eta_1 + \eta_2)(1 + \chi) + 1} \quad (5)$$

where $\chi = Y_f/Y_s$, $\eta_1 = d_{f1}/d_s$ and $\eta_2 = d_{f2}/d_s$.

We used Eq. (5) to calculate the value of the compressive strain in the channel of our TFTs for each bending radius R . We calculate $\epsilon_{surface}$ for two structures: one with the back SiN_x layer, i.e., the as-fabricated sandwich structure of Fig. 1(a), and the other without this SiN_x layer, as employed in the bending experiments, Fig. 1(b). Table 1 summarizes the results. Removing the back SiN_x layer makes the substrate more compliant and reduces the strain in the TFT channel area by a factor of ~ 2 . From experiment and the calculated strain we conclude that TFTs on 25 μm thick Kapton continue to function, without any substantial change in their electrical performance, down to $R = 0.5$ mm, which corresponds to a bending strain of $\sim 1\%$. Previous experiments with bending TFTs on 25 μm thick steel foil (a stiff substrate) have shown that a-Si:H TFTs can be strained by $\sim 0.5\%$ before failing mechanically at a radius of curvature R of ~ 2 mm [10]. This lower attainable strain in TFTs on steel may be caused by film delamination due to inadequate adhesion between the substrate and the TFT structure.

Table 1. Bending strain $\epsilon_{surface}$ in the channel area of the TFT calculated from Eq. (5). ($d_s = 25 \mu\text{m}$, $Y_f = 200$ GPa, $Y_s = 5$ GPa)

R (mm)	Strain (%)	Strain (%)
	(sandwich structure)	(back SiN_x layer removed)
0.25	4.15	2.20
0.5	2.08	1.10
1	1.04	0.55
1.5	0.69	0.37
2	0.52	0.27
2.5	0.42	0.22
3	0.35	0.18
4	0.26	0.14

known function of z . No external force is applied in the plane of the foil. Force balance requires that

$$\int \sigma_x dz = 0 \quad (3)$$

Hooke's law relates the stress σ to the strain ϵ via

$$\sigma_x = Y\epsilon_x \quad (4)$$

By inserting Eqs. (2) and (4) into Eq. (3) and integrating we obtain the position of the neutral plane with respect to either of the top

SUMMARY

Earlier experiments with bending TFTs on 25- μm thick steel foil (a stiff substrate) have shown that a-Si:H TFTs can be strained by at least 0.5 % before failing mechanically at a radius of curvature R of ~ 2 mm [10]. Our present observation that TFTs made on the same thickness of Kapton foil (a compliant substrate) function down to $R = 0.5$ mm provides direct evidence for the strain-relieving effect of a compliant substrate. This observation agrees with the theoretical prediction that the strain in the plane of the circuit can be reduced by a factor of up to 5 when going from stiff to a compliant substrate [9]. Thus both experiment and theory suggest that nearly-foldable thin-film circuits are a realistic prospect.

ACKNOWLEDGMENTS

We gratefully acknowledge support from the DARPA HDS program and thank DuPont for donating Kapton E foils.

REFERENCES

1. G.N. Parsons, C.S. Yang, C.B. Arthur, T.M. Klein, and L. Smith, in *Flat Panel Display Materials - 1998*, edited by G.N. Parsons, C.C. Tsai, T.S. Fahlen, and C.H. Seager, (Mat. Res. Soc. Symp. Proc. **508**, Pittsburgh, PA, 1998), pp. 19-24.
2. H. Gleskova, S. Wagner and Z. Suo, in *Flat Panel Display Materials - 1998*, edited by G.N. Parsons, C.C. Tsai, T.S. Fahlen, and C.H. Seager, (Mat. Res. Soc. Symp. Proc. **508**, Pittsburgh, PA, 1998), pp. 73-78.
3. J.N. Sandoe, *Digest of Technical Papers of the Society for Information Display*, Vol. **29**, 1998, pp. 293-296.
4. E. Lueder, M. Muecke, S. Polach, *Proc. of the Int. Display Research Conf., Asia Display 98*, 1998, pp. 173-177.
5. A. Constant, S.G. Burns, H. Shanks, C. Gruber, A. Landin, D. Schmidt, C. Thielen, F. Olympie, T. Schumacher, and J. Cobbs, *The Electrochemical Society Proceedings*, Vol. **94-35**, pp. 392-400.
6. S.G. Burns, H. Shanks, A. Constant, C. Gruber, D. Schmidt, A. Landin, and F. Olympie, *The Electrochemical Society Proceedings*, Vol. **96-23**, pp. 382-390.
7. S. D. Theiss, P. G. Carey, P.M. Smith, P. Wickboldt, T.W. Sigmon, Y.J. Tung, and T.-J. King, *IEEE Int. Electron Devices Meeting 1998, Technical Digest*, pp. 257-260.
8. D.B. Thomasson, M. Bonse, J.R. Huang, C.R. Wronski, and T.N. Jackson, *IEEE Int. Electron Devices Meeting 1998, Technical Digest*, pp. 253-256.
9. Z. Suo, E.Y. Ma, H. Gleskova, and S. Wagner, *Appl. Phys. Lett.* **74**, 1999, pp. 1177-1179.
10. E.Y. Ma and S. Wagner, in *Flat Panel Display Materials - 1998*, edited by G.N. Parsons, C.C. Tsai, T.S. Fahlen, and C.H. Seager, (Mat. Res. Soc. Symp. Proc. **508**, Pittsburgh, PA, 1998), pp. 13-18.